

Electric field control of the magnetic state in BiFeO₃ single crystals

Seungsu Lee,¹ W. Ratcliff II,² S-W. Cheong,¹ and V. Kiryukhin^{1,a)}

¹Rutgers Center for Emergent Materials and Department of Physics and Astronomy, Rutgers University, Piscataway, New Jersey 08854, USA

²NIST Center for Neutron Research, NIST, Gaithersburg, Maryland 20899, USA

(Received 10 April 2008; accepted 26 April 2008; published online 16 May 2008)

Single crystals of multiferroic BiFeO₃ were investigated using neutron scattering. Application of an electric field reversibly switches ferroelastic domains, inducing changes in the magnetic structure which follows rotation of the structural domains. In addition, electric fields can be used to control the populations of the equivalent magnetic domains within a single ferroelastic domain, possibly via field-induced strain. © 2008 American Institute of Physics. [DOI: 10.1063/1.2930678]

Multiferroics provide opportunities for devices with unique functionalities utilizing the coupling between order parameters.^{1,2} Controlling magnetism with an external electric field is one of the most important of these opportunities. Unfortunately, until recently, no significant effects of an electric field on magnetic structure have been observed in single-phase multiferroics.³ This changed with the important discovery of room-temperature magnetoelectric (ME) coupling in thin films of BiFeO₃, in which spins are strongly coupled to ferroelastic domains.⁴ Now, studies of single crystals are required to uncover *intrinsic* properties of this unique material. They have direct relevance for thin films whose properties are strongly affected by extrinsic strain.¹ In addition, demonstration of electric field induced changes in the magnetic structure by direct methods (neutron scattering) until now was lacking for BiFeO₃.

Arguably, BiFeO₃ is the most extensively studied multiferroic due to its large polarization and room-temperature multiferroicity.⁵ However, studies of large (approximately millimeter sized) single crystals appeared only recently,⁶ and many basic properties of single crystals are still unknown. The ferroelectric phase ($T < T_C \approx 850$ °C) exhibits the rhombohedral $R3c$ structure with a pseudocubic perovskite unit cell ($a \approx 3.96$ Å, $\alpha \approx 89.4$ °) elongated along the (111) direction.⁷ The pseudocubic notation is used in this paper. The unique (111) direction coincides with the ferroelectric polarization direction, resulting in four structural variants based on the four body diagonals of the pseudocubic cell. For $T < T_N \approx 370$ °C, Fe spins order antiferromagnetically⁸ in the G -type structure locally, with a long-range ($\lambda \approx 620$ Å) modulation, believed to be cycloidal based on neutron diffraction results.^{7,9} The modulation wavevector is $\tau_1 = (\delta, -\delta, 0)$, with $\delta = 0.0045$. Wavevectors $\tau_2 = (\delta, 0, -\delta)$ and $\tau_3 = (0, -\delta, \delta)$ are equivalent by symmetry, giving three propagation directions, each perpendicular to the electric polarization and τ .

Single crystals of BiFeO₃ were grown using a Bi₂O₃ flux. Two crystals, both $3 \times 2 \times 1$ mm³, were chosen for the experiment. Sample 2 had two parallel gold contacts evaporated onto the largest sample faces for application of an electric field in the cubic direction. Experiments were carried out at $T = 50$ K on BT-9 triple-axis spectrometer at NIST Center

for Neutron Research at an energy of 14.7 meV, with collimations 40-10-S-40-80.

Both crystals were found to consist of a single ferroelastic domain with one unique (111) direction. Figure 1(a) shows $(h, -h, 0)$ scan at the $(\frac{1}{2}, \frac{1}{2}, \frac{1}{2}) \pm \tau$ magnetic peak in the $(h, 2l-h, l)$ plane for sample 1, in which the best peak resolution is achieved. Signal at both $\pm\delta$ and $\pm\delta/2$ positions is present. The inset shows the former signal results from the τ_1 magnetic domain, while the latter from the τ_2 or τ_3 domains. The out-of-scattering-plane domains τ_2 and τ_3 are observed due to broad out-of-plane instrumental resolution. Thus, equivalent magnetic domains are present in the sample. The domain population can be estimated from the integrated intensity of the corresponding peaks. From the fit shown in Fig. 1(a), we obtain $\delta = 0.0042(2)$, and volume fractions of 0.6 and 0.4 for the τ_1 and $\tau_2 + \tau_3$ domains, respectively.

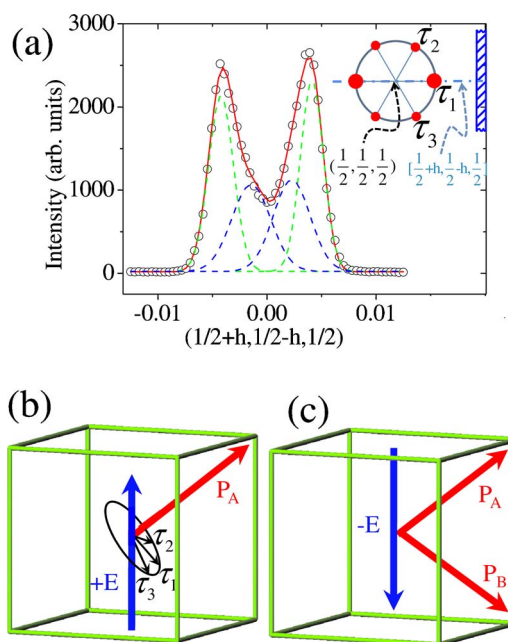


FIG. 1. (Color online) (a) $(h, -h, \frac{1}{2})$ scan at the $(\frac{1}{2}, \frac{1}{2}, \frac{1}{2}) \pm \tau$ magnetic peak in the $(h, 2l-h, l)$ plane. Dashed lines show peaks in the $\pm\delta$ and $\pm\delta/2$ positions, solid line is the final fit. The inset shows $(\frac{1}{2}, \frac{1}{2}, \frac{1}{2}) \pm \tau$ peaks in the $(h, k, -h-k)$ plane. The projection of the experimental scattering plane is shown with dot-dashed line. Dashed rectangle represents experimental resolution. (b) and (c) show the electric field and polarization vectors of domains A and B in the single domain scenario discussed in the text for $E > 0$ and $E < 0$, respectively.

^{a)}Electronic mail: vkir@physics.rutgers.edu.

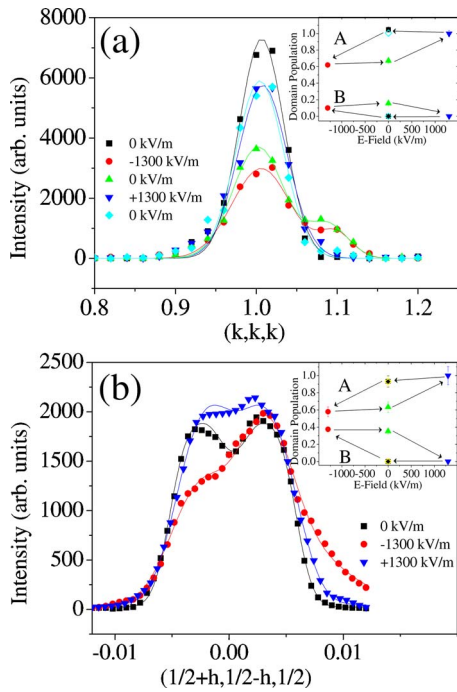


FIG. 2. (Color online) (a) Scans through the (111) peak (domain A) and (1-11) or equivalent peak (domain B). (b) Scans through the $(\frac{1}{2}, \frac{1}{2}, \frac{1}{2}) \pm \tau$ (domain A), and $(\frac{1}{2}, -\frac{1}{2}, \frac{1}{2}) \pm \tau$ or equivalent (domain B) magnetic peaks. In (b), zero-field data are shown only for the as-prepared sample for clarity. Solid lines are fits, as discussed in the text. The insets show ferroelastic domain populations for various applied electric fields. Electric fields were applied in the sequence shown in the legend. Error bars represent one standard deviation.

Application of an electric field along the negative (010) direction ($E = -1.3$ MV/m) in sample 2 results in appearance of a different ferroelastic domain. Figure 2(a) shows that the field diminishes the intensity of the (111) structural peak, while a new peak, at scattering angle corresponding to the longer (1-11) wavevector appears in the vicinity. Thus, a ferroelastic domain (domain B) in which the unique (111) direction does not coincide with the (111) body diagonal of the original domain (A) emerges. The field-induced change is largely reversible: application of positive field destroys domain B, and the cycle is repeatable. The domain populations obtained from integrated peak intensities form hysteresis loops, as shown in Fig. 2(a) (inset). Some intensity from domain B is missing, indicating that our scans slightly miss the maximum of the domain B peak. Emergence of domain B coincides with appearance of magnetic signal near the $(\frac{1}{2}, \frac{1}{2}, \frac{1}{2})$ position of domain A that cannot be described by $(\frac{1}{2}, \frac{1}{2}, \frac{1}{2}) \pm \tau$ peaks [see Fig. 2(b)]. The extra intensity appears at larger scattering angle, which is consistent with the appearance of the magnetic signal associated with the $(\frac{1}{2}, -\frac{1}{2}, \frac{1}{2}) \pm \tau$ (or equivalent) peak of domain B. Such signal must appear if the spins keep their orientation with respect to the crystal lattice. To estimate this signal, the domain A intensity was approximated by its zero-field shape, fitted at its lower-angle wing, and subtracted from the total signal. The remaining intensity forms a broad peak with center of mass matching the scattering angle of the $(\frac{1}{2}, -\frac{1}{2}, \frac{1}{2})$ peak. Thus, our data strongly suggest that the newly observed intensity comes from domain B. Consistently, it disappears in positive electric fields, when domain B is destroyed. The integrated intensities (volume fractions) of the domain A and B mag-

netic signals, determined by the above procedure with domain B intensity described by a Gaussian peak, are shown in Fig. 2(b) (inset). The observed hysteresis loops agree qualitatively with the ferroelastic domain populations of Fig. 2(a). We note that a rotation (but not full hysteresis loops) of the magnetic spiral by an electric field was very recently reported in a preprint by Lebeugle *et al.*⁹

In positive fields, only ferroelastic domain A is present, and the magnetic signal is well described by $(\frac{1}{2}, \frac{1}{2}, \frac{1}{2}) \pm \tau$ peaks. However, the data of Fig. 2(b) clearly show that the signal of the $\tau_2 + \tau_3$ domains ($h = \frac{1}{2} \pm \delta/2$) is stronger than that in the as-prepared sample in zero field. Fits similar to those shown in Fig. 1(a) reveal that the volume population of the $\tau_2 + \tau_3$ domain increases from 0.80 in the as-prepared state to 0.85 for $E = 1.3$ MV/m, with matching changes in the τ_1 domain population. The same effect occurs if $E = 1.3$ MV/m is applied directly to the as-prepared state (without intervening application of negative field). The as-prepared state can be restored by room temperature annealing.

The obtained results demonstrate that the magnetic state in BiFeO₃ is controllable by an electric field in two very different ways. First, an electric field can induce a new ferroelastic domain with its own unique (111) direction by coupling to ferroelectric polarization. The magnetic structure exhibits corresponding changes that are consistent with rigid coupling between the spins and crystal lattice. If the magnetic structure is a spiral, the electric field should flip the spiral plane. In our sample, the original ferroelastic domain can be restored by the opposite electric field and, therefore, the magnetic state can be switched reversibly. The observed behavior is strongly asymmetric with respect to the sign of the electric field: domain B is only induced for $E < 0$. This indicates that single ferroelectric domain is dominant in the as-prepared sample. In this case, application of an electric field in the cubic direction at an acute angle to the polarization [Fig. 1(b)] should not produce any structural change because of the elastic energy costs. When the field is reversed, a new ferroelastic domain is expected to appear. Polarization direction in this domain, obtained from elastic energy considerations,¹⁰ is shown in Fig. 1(c). Our data are consistent with this scenario, with $E > 0$ corresponding to the geometry of Fig. 1(b). This also agrees with our preliminary piezoresponse force microscopy measurements (not shown) which do not show any domain boundaries in the sample.

Second, changes in the populations of the equivalent magnetic domains τ_1 , τ_2 , and τ_3 within a single ferroelastic domain can be induced. The probable mechanism underlying this effect is field-induced uniaxial elastic strain ξ which lifts the threefold symmetry that makes the domains equivalent. In our experiments, $\xi = d_{33}E \approx 5 \times 10^{-5}$ ($d_{33} = 10 - 50$ pm/V is the piezoelectric coefficient^{6,11}) and, therefore, the magnetic domains are quite sensitive to strain.

Strong ME effects, related to the ferroelastic domain switching reported here, were found previously in thin films,⁴ in which the magnetic cycloid is absent due to epitaxial strain, and spins are thought to be almost collinear.⁵ It was suggested that the ME effects should be much smaller in single crystals because of the cancellation of the linear ME coupling in the cycloid structure.¹² Contrarily, our results clearly demonstrate a strong, intrinsic coupling between magnetism and ferroelectricity in BiFeO₃. Together with the remarkable sensitivity of the magnetic domains to strain, this

should be of importance to studies of thin films, in which strain can be controlled.

In conclusion, our results reveal a strong, intrinsic ME coupling in BiFeO₃. Magnetism can be controlled by an electric field through (i) reversible ferroelectric domain switching in which spins follow the lattice (as also observed in thin films) and (ii) strain-induced redistribution of the occupations of equivalent magnetic domains (unique to single crystals).

This work was supported by the NSF under Grant Nos. DMR-0520471 and DMR-0704487.

¹R. Ramesh and N. A. Spaldin, *Nat. Mater.* **6**, 21 (2007).

²S.-W. Cheong and M. Mostovoy, *Nat. Mater.* **6**, 13 (2007).

³T. Lottermoser, T. Tonkai, U. Amann, D. Hohlwein, J. Ihringer, and M. Feibig, *Nature (London)* **430**, 541 (2004).

⁴T. Zhao, A. Scholl, F. Zavaliche, K. Lee, M. Barry, A. Doran, M. P. Cruz,

Y. H. Chu, C. Ederer, N. A. Spaldin, R. R. Das, D. M. Kim, S. H. Baek, C. B. Eom, and R. Ramesh, *Nat. Mater.* **5**, 823 (2006).

⁵Y.-H. Chu, L. W. Martin, M. B. Holcomb, and R. Ramesh, *Mater. Today* **10**, 16 (2007).

⁶D. Lebeugle, D. Colson, A. Forget, M. Viret, P. Bonville, J. F. Marucco, and S. Fusil, *Phys. Rev. B* **76**, 024116 (2007).

⁷I. Sosnovska, T. Peterlin-Neumaier, and E. Steichele, *J. Phys. C* **15**, 4835 (1982).

⁸J. M. Moreau, C. Michel, R. Gerson, and W. J. James, *J. Phys. Chem. Solids* **32**, 1315 (1971).

⁹D. Lebeugle, D. Colson, A. Forget, M. Viret, A. M. Bataille, and A. Gukasov, arXiv:0802.2915.

¹⁰S. K. Streffer, C. B. Parker, A. E. Romanov, M. J. Lefevre, L. Zhao, J. S. Speck, W. Pompe, C. M. Foster, and G. R. Bai, *J. Appl. Phys.* **83**, 2742 (1998).

¹¹S. K. Singh, R. Ueno, H. Funakubo, H. Uchida, S. Koda, and H. Ishiwara, *Jpn. J. Appl. Phys., Part 1* **44**, 8525 (2005).

¹²A. M. Kadomtseva, A. K. Zvezdin, Yu. F. Popov, A. P. Pyatakov, and G. P. Vorob'ev, *JETP Lett.* **11**, 571 (2004).